Variational Transition State Theory and Tunneling Calculations of Potential Energy Surface Effects on the Reaction of O(

CHAPTER *in* SYMPOSIUM (INTERNATIONAL) ON COMBUSTION · JANUARY 1984

DOI: 10.1016/S0082-0784(85)80547-6

3 AUTHORS, INCLUDING:

Donald Truhlar
University of Minnesota Twin Cities
1,342 PUBLICATIONS **81,158** CITATIONS
SEE PROFILE

Bruce C Garrett
Pacific Northwest National Laboratory
296 PUBLICATIONS **11,928** CITATIONS
SEE PROFILE

"Variational Transition State Theory and Tunneling Calculations of Potential Energy Surface Effects on the Reaction of $O(^3P)$ with H_2," D. G. Truhlar, K. Runge, and B. C. Garrett, in Twentieth Symposium (international) on Combustion (Combustion Institute, Pittsburgh, 1984), pp. 585-593. See also discussion remarks: pp. 593-594.

Twentieth Symposium (International) on Combustion/The Combustion Institute, 1984/pp. 585–594

VARIATIONAL TRANSITION STATE THEORY AND TUNNELING CALCULATIONS OF POTENTIAL ENERGY SURFACE EFFECTS ON THE REACTION OF $O(^3P)$ WITH H_2

DONALD G. TRUHLAR AND KEITH RUNGE
Department of Chemistry
University of Minnesota
Minneapolis, Minnesota 55455

AND

BRUCE C. GARRETT
Chemical Dynamics Corporation
1550 W. Henderson Road
Columbus, Ohio 43220

Variational transition state theory with adiabatic and least-action ground-state transmission coefficients is applied to calculate reaction rates for $O(^3P) + H_2 \rightarrow OH + H$ in both collinear and three-dimensional worlds for temperatures of 200–1400 K. Five different potential energy surfaces are considered. The collinear studies are used to assess the accuracy of the dynamical and energetic approximations, which include the no-recrossing assumption of generalized transition state theory, semiclassical methods for tunneling calculations, and a Morse approximation for quantizing the generalized-transition-state stretching vibrations. Although the potential energy surfaces show wide differences in behavior, the calculations with least-action ground-state transmission coefficients agree with the accurate quantal results within a factor of 2.8 in all cases. We find that the three-dimensional reaction is dominated by tunneling at room temperature and nearby for all five surfaces. For the calculations on the most accurate ab initio potential energy surface, 60% of the ground-state reaction proceeds by tunneling even at 400 K. The tunneling fractions rise dramatically as the temperature is lowered. The calculations show that quantitative estimation of the tunneling effects requires consideration of reaction-path curvature and of tunneling paths that deviate from the minimum energy path.

1. Introduction

$O + H_2$ is one of the simplest reactions important in combustion. In this paper we calculate rate constants for this reaction by variational transition state theory (VTST) with ground-state (G) transmission coefficients (VTST/G). We perform the calculations with five different potential energy surfaces, and we study the importance of optimizing the location of the generalized transition state, of tunneling, and of reaction-path curvature and bending effects on the tunneling coefficients. We also study the sensitivity of various features of the results to the choice of potential surface.

2. Potential Energy Surfaces

Wagner, Bowman, Schatz, and coworkers have presented a series of comparative studies of $O(^3P) + H_2$ dynamics on several potential energy surfaces,[1–8] and they calculated accurate quantal collinear reaction probabilities and rate constants for five of these surfaces. Since the accurate quantal results provide an informative test of approximate dynamical methods we will use the same five collinear potential surfaces here. They are the surfaces of Johnson and Winter[9] (JW) and Schinke and Lester[10] (SL), rotated-Morse-oscillator (RMOS) fits[2,3] to the diatomics-in-molecules surface of Whitlock *et al.*[11] and to the polarization configuration interaction calculations of Walch and coworkers,[1,12] and a modified surface[8] that forces the latter fit to have the correct reaction endoergicity. The last three surfaces are denoted DIM-RMOS, POLCI-RMOS, and ModPOLCI-RMOS. Wagner and coworkers did not perform full dynamical calculations for three-dimensional reactions; they performed conventional transition state theory (TST) calculations with transmission coefficients based on collinear dynamical

calculations or on the Wigner lowest-order quantal correction for a quadratic approximation to the potential surface. The only pieces of information about the potential surfaces for noncollinear geometries that they used were the bending force constants at the saddlepoints. For our present calculations we require bending force constants along the entire lengths of the minimum-energy paths. The JW and SL surfaces are defined for all geometries, and we use them unaltered. The RMOS surfaces are defined only for collinear geometries, and we extended them to surfaces for three-dimensional reaction by the anti-Morse bend (AB) model[13-15] described previously. The parameters of the bend potential were the same for all three surfaces, namely, in the notation of ref. 15: $\gamma = 0.4131$, $D_e^{AC} = 106.56$ kcal/mol, $a_M^{AC} = 2.07942$ Å^{-1}, and $r_e^{AC} = 0.96966$ Å. The latter three parameters are accurate values for OH[16] and γ was adjusted such that the saddlepoint harmonic bending frequency (for the $1^2A''$ ground electronic state) on the ModPOLCI-RMOS/AB surface agrees with the ab initio value.[1] The DIM-RMOS/AB, POLCI-RMOS/AB, and ModPOLCI-RMOS/AB surfaces will be denoted D, P, and M, respectively.

3. Methods

The VTST/G approximation to the rate constant has two factors.[17] The first is the hybrid VTST part in which the rate constant is calculated with reaction-coordinate motion treated classically and other degrees of freedom quantized under the assumption that the equilibrium one-way flux in the product direction through a generalized transition state equals the net reactive flux.[18] This assumption involves both an equilibrium assumption, that reactants (and hence systems crossing the transition state in the product direction) are in local equilibrium, and also a no-recrossing assumption, that systems do not cross through the generalized transition state more than once before being equilibrated as reactants or products. The generalized transition state is orthogonal to a reaction path and its location along this path is variationally optimized to minimize the equilibrium one-way flux for a given ensemble, of which we consider two. Microcanonical variational theory (μVT) involves optimizing the generalized transition state for each total energy.[18] The microcanonical results are thermally averaged to calculate the rate constant at a temperature. Improved canonical variational theory (ICVT) involves optimizing the generalized transition state for each temperature for a canonical ensemble truncated at the μVT threshold energy and also enforcing the μVT threshold energy as the lower energy limit in the thermal average.[17] In the present study we performed both μVT and ICVT calculations for the collinear reactions but only ICVT calculations for the three-dimensional reaction.

The second factor in a VTST/G calculation is a ground-state transmission coefficient, which is the ratio of a thermally averaged approximate quantal or semiclassical reaction probability for ground-state reactants to the thermally averaged ground-state reaction probability implied by μVT or ICVT with classical reaction-coordinate motion.[17] The ground-state transmission coefficient accounts for quantal effects on the reaction-coordinate motion, and we consider three different approximations: MEPSAG, SCTSAG, and LAG. The first two methods are semiclassical adiabatic approximations based on dominant tunneling paths and the adiabatic approximation for the effective potential along these paths. The MEPSAG method involves tunneling along the minimum-energy path with no account taken of reaction-path curvature;[17] the SCTSAG method treats reaction-path curvature in the small-curvature approximation, which uses an effective reduced mass to account for the tendency of the dominant tunneling path to be located on the concave side of the minimum energy path.[19] The LAG transmission coefficient is based on a more general approximation that involves an approximate least-action variational principle to optimize a series of tunneling paths; close to the reaction path the effective potential along the tunneling paths is modelled by the adiabatic approximation using the local vibrational potential; but far from the reaction path it is computed directly from the potential surface in cartesian coordinates.[20]

For collinear collisions we also calculate small-curvature approximation semiclassical adiabatic microcanonical reaction probabilities. These are defined by

$$P^{SCSA}(E) = [N^R(E)]^{-1} \sum_{n=0}^{N^R(E)} P^{SCSA}(n,E) \qquad (1)$$

where E is total energy, $N^R(E)$ is the number of energetically open vibrational states of the reactant, n is vibrational quantum number, and $P^{SCSA}(n,E)$ is the small-curvature semiclassical adiabatic approximation to the state-selected reaction probability for initial state n and total energy E. We measure total energy with respect to the classical equilibrium potential energy of O infinitely separated from H_2. The accurate quantal microcanonical reaction probabilities P(E) are computed analogously to eq. (1) but with accurate quantal state-selected reaction probabilities $P(n,E)$ replacing $P^{SCSA}(n,E)$.

The methods and equations used for the VTST/G calculations have all been explained previously.[17-22] Reaction paths and their curvatures are computed by following the gradient of the potential energy surface in mass-scaled coordinates in both

directions from the saddlepoint.[17,18,22] For all five surfaces studied here the saddlepoints and reaction paths correspond to collinear geometries. Local vibrational potentials orthogonal to the reaction path are computed by the Morse I approximation for stretches[18] and by a Taylor series truncated at harmonic and quartic terms for bends.[17,21,22] Partition functions are computed by summing independent-mode-approximation Boltzmann factors up to the dissociation limit (or convergence if it occurs first).

For collinear reactions, as usual, all theoretical rate constants refer to a hypothetical world with one specified nondegenerate potential energy surface. For three-dimensional reactions, multiple surface effects are treated, as usual, by assuming that only the ground electronic surface ($1^3A''$) is reactive. We include spin-orbit splitting in $O(^3P)$ but neglect it in the generalized transition states. Thus the electronic partition function is 3 for all generalized transition states and is computed from the $J = 2,1,0$ states for the $O(^3P)$ reactant. The multiple-surface coefficient computed this way varies from 0.487 to 200 K to 0.333 in the high-temperature limit.

A correction for the nonzero reaction probability on the first excited potential energy surface ($1^3A'$) may be estimated[5] by conventional transition state theory with harmonic bends by using the *ab initio* harmonic bending frequencies for the $^3A''$ and $^3A'$ saddlepoints; this yields a correction that increases from 1.06 at room temperature to 1.22 at 1400 K. We do not include this correction in our results.

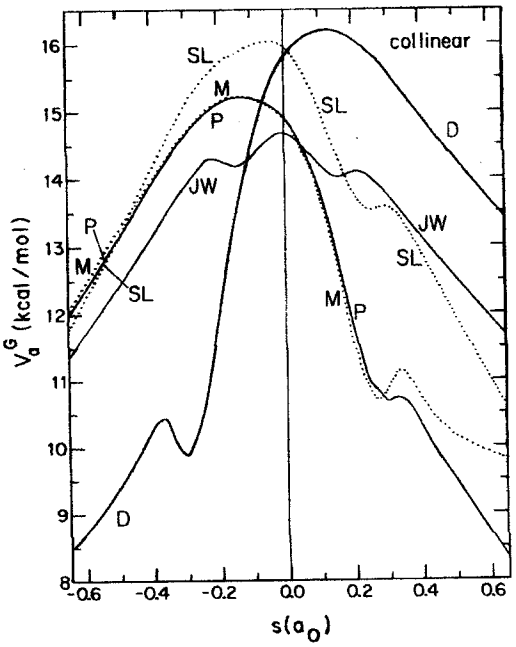

FIG. 1. Vibrationally adiabatic ground-state potential curves as functions of reaction coordinate (distance along the reaction path through mass-scaled coordinates for a reduced mass of 3263.2 u) for collinear reaction on five potential energy surfaces. The thin vertical axis denotes the saddlepoint location, which is assigned the location $s = 0$ in all cases.

4. Results and Discussion

4.1 *Collinear Reaction*

Figure 1 shows the vibrationally adiabatic ground-state potential curves for collinear reaction on all five surfaces. These curves are obtained by adding the local vibrational zero-point energy to the potential energy at each point along the reaction path.[17,18] The MEPSAG transmission coefficients are based on one-dimensional tunneling through these barriers with a constant reduced mass corresponding to the correct asymptotic reduced mass for $O + H_2$, namely 3263.2 u. The small-curvature ground-state transmission coefficients involve s-dependent reduced masses which are lower in regions of nonzero reaction-path curvature. The least-action transmission coefficients are based on the vibrationally adiabatic model only at the beginning and end of the tunneling process. The resulting thermally averaged transmission coefficients are tabulated in Table I. This table shows several interesting features: (i) Reaction-path-curvature plays a large role in the tunneling processes, as evidenced by the fact that the SCTSAG and LAG tranmission coefficients exceed the MEPSAG ones by factors as large as 17 and 29, respectively. (ii) The transmission coefficients are very large at room temperature and below, indicating that almost all the reaction proceeds by tunneling. (iii) Changing the potential energy surface makes a large difference in both the transmission coefficients themselves and the effect of reaction-path curvature on the transmission coefficients.

Changing the potential surfaces also affects the classical-reaction-coordinate part of the calculation, i.e., the hybrid VTST rate constants. The fact that the vibrationally adiabatic ground-state potential curves in Fig. 1 do not peak at the saddlepoints for four of the surfaces is an indication that variational optimization of the location of the generalized transition states will have an effect on the hybrid rate constants in these four cases.[18,23,24] We found that for all five surfaces the hybrid VTST collinear rate constants calculated by μVT and ICVT agreed within 2%, and usually much better, over the whole temperature range studied. Thus we will present in detail only the results obtained by the simpler ICVT calculations. Table II shows that variational optimization of the location of the generalized transition state lowers the rate constant by various amounts

TABLE I
Transmission coefficients

T(K)	Collinear			Three-dimensional		
	MEPSAG	SCTSAG	LAG	MEPSAG	SCTSAG	LAG
			JW Surface			
200	4.08	25.3	54.3	9.11	134.5	426.5
300	1.84	4.63	7.55	2.50	10.3	20.0
400	1.41	2.49	3.50	1.66	3.98	6.06
600	1.17	1.57	1.91	1.26	1.96	2.41
			SL Surface			
200	18.7	314.7	545.4	28.1	704.1	1581.9
300	3.24	13.4	14.5	3.60	17.8	19.9
400	1.88	4.40	4.04	1.96	5.03	4.45
600	1.31	1.99	1.76	1.33	2.09	1.76
			Surface D			
200	17.5	83.9	41.8	29.2	194.0	115.3
300	3.08	7.28	4.03	3.62	10.3	5.48
400	1.82	3.12	2.05	1.97	3.78	2.33
600	1.29	1.71	1.35	1.33	1.86	1.41
			Surface P			
200	21.3	247.6	250.8	32.3	510.0	611.4
300	3.03	10.0	6.42	3.46	13.4	8.80
400	1.78	3.57	2.35	1.89	4.07	2.64
600	1.27	1.79	1.39	1.31	1.91	1.44
			Surface M			
200	19.9	180.1	253.5	30.0	358.1	604.7
300	3.02	9.53	7.10	3.45	12.6	10.1
400	1.78	3.52	2.45	1.90	4.07	2.82
600	1.27	1.78	1.40	1.31	1.90	1.46

ranging from less than 1% of the JW surface at low temperature to over a factor of two for surfaces P and M at low temperature. At 1400 K the effect is less dependent on surface, ranging from a factor of 1.22 to a factor of 1.35 in all cases.

Table II also compares the VTST/SCTSAG and VTST/LAG rate constants to the accurate[7] quantal ones. Compared to the large sizes of the quantal tunneling corrections as well as the large surface dependance of both the tunneling corrections and the variational optimization effects, the ratios of the approximate rate constants to the accurate ones are for the most part remarkably close to unity. In some cases the SCTSAG transmission coefficient yields more accurate results while in other cases the LAG transmission coefficient does. Overall the LAG values appear slightly more accurate.

The trends in accuracy may be understood by considering Figs. 2–4, which show the small-curvature-approximation semiclassical adiabatic (SCSA) microcanonical reaction probabilities[18] and compare them to the accurate quantal ones, which we computed from the results in Ref. 7. Since μVT reduces to the adiabatic theory of reactions when the reaction coordinate is treated classically, the SCSA results in Figs. 2–4 may be considered to represent a microcanonical generalization of VTST with a small curvature-approximation semiclassical adiabatic transmission coefficient. In particular, since low energies and the ground vibrational state dominate the thermal averages for cases considered here, a thermal average of the $P^{SCSA}(E)$ curves would yield results very close to $k^{ICVT/SCTSAG}(T)$. The integrands of the thermal averages in the SCTSAG transmission coefficients give an indication of the most important energy regions controlling the rate constants at various temperatures. These peaks are given in the figure captions, and they provide the basis for some of the conclusions drawn in the following.

For the JW surface, $P^{SCSA}(E)$ is qualitatively correct over the whole relevant range of E. The underestimates of the rate constants by the approximate calculations (Table II) are a result of

TABLE II
Ratios of collinear rate constants

T(K)	$k^{\ddagger}/k^{ICVT}$	$k^{ICVT/SCTSAG}/k$	$k^{ICVT/LAG}/k$
		JW Surface	
200	1.00	0.42	0.91
300	1.00	0.49	0.80
400	1.01	0.55	0.77
600	1.03	0.64	0.78
1000	1.12	0.76	0.84
1400	1.22	0.86	0.91
		SL Surface	
200	1.23	1.04	1.80
300	1.15	0.82	0.89
400	1.11	0.81	0.75
600	1.10	0.87	0.77
1000	1.16	0.96	0.88
1400	1.25	1.03	0.97
		Surface D	
200	2.78	1.44	0.72
300	1.98	1.81	1.00
400	1.67	1.96	1.29
600	1.43	2.29	1.81
1000	1.32	2.53	2.26
1400	1.33	2.97	2.76
		Surface P	
200	2.18	0.69	0.70
300	1.68	0.94	0.60
400	1.48	1.08	0.71
600	1.33	1.35	1.05
1000	1.29	1.21	1.07
1400	1.33	1.24	1.14
		Surface M	
200	2.35	0.53	0.75
300	1.77	0.78	0.58
400	1.54	1.00	0.70
600	1.36	1.27	1.00
1000	1.31	1.44	1.27
1400	1.35	1.50	1.39

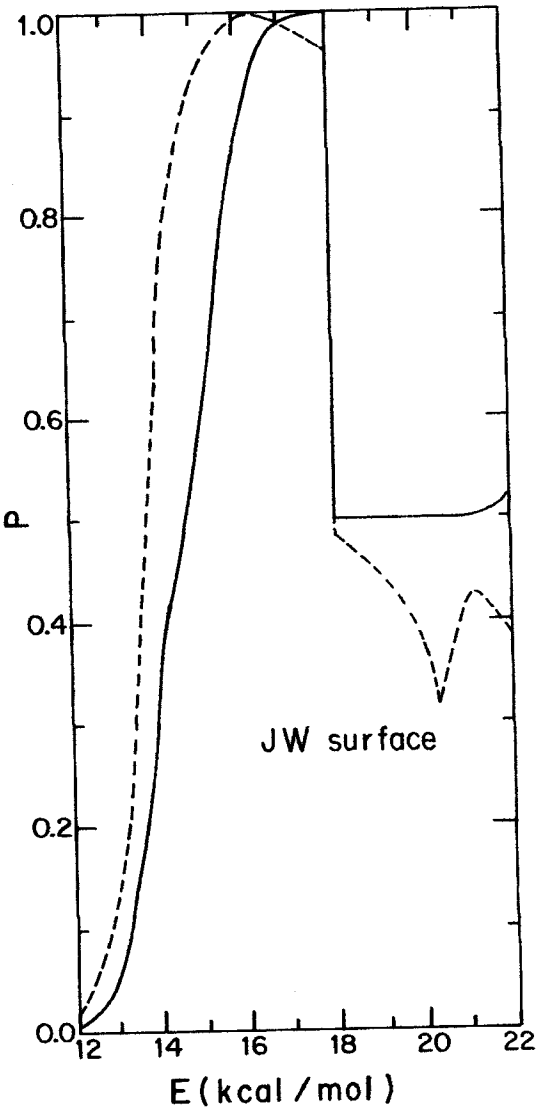

FIG. 2. Reaction probabilities for a microcanonical ensemble as a function of total energy for the collinear reaction on the JW potential energy surface. The dashed curve represents the accurate results of Lee *et al.* (ref. 7); the solid curve represents the present calculations by the small-curvature-approximation semiclassical adiabatic approximation. The integrands of the thermal averages in the SCTSAG transmission coefficients for 200, 300, and 800 K peak at 12.7, 13.5, and 14.3 kcal/mol, respectively.

underestimating the low-E tunneling probabilities. For the ICVT/LAG calculations the errors are very small.

For the SL surface the results are similar except that the approximate tunneling calculations appear to overestimate the accurate probabilities for E < 13 kcal/mol. This has a significant effect on the rates only at 200 K.

For surface D the trends are different. Here there appears to be significant recrossing since the accurate reaction probabilities are overestimated by over a factor of 3 at the energy of the peak in the 800 K thermal average. This results in significant overestimates by $k^{ICVT/SCTSAG}$. This is a rather unusual case; although we have previously studied very many collinear reactions, only the F + H_2 reaction

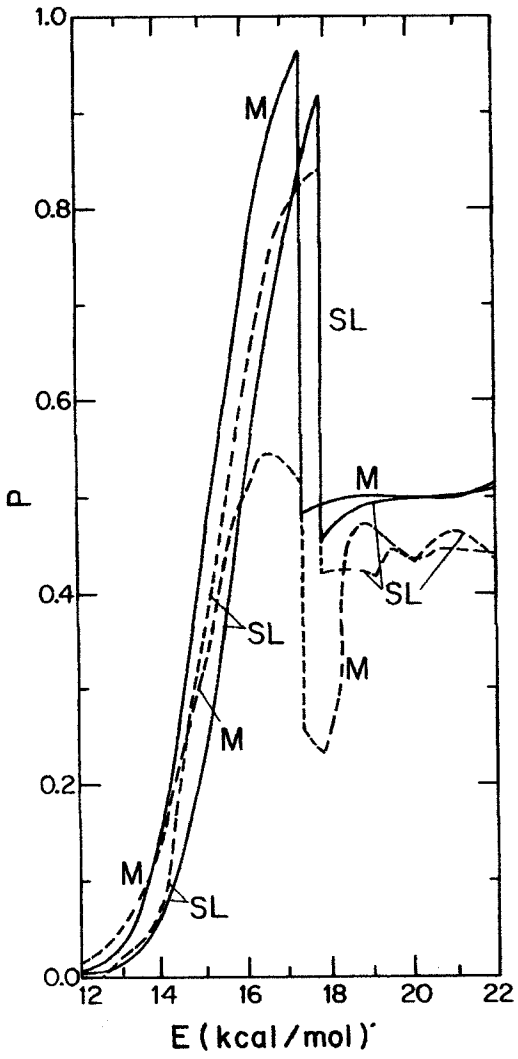

FIG. 3. Same as Fig. 2 except for the SL potential energy surface, for which the integrand peaks are at 11.9, 13.6, and 15.9 kcal/mol, and for potential energy surface M, for which the integrand peaks are at 10.9, 13.2, and 15.1 kcal/mol.

(and its isotopic analog F + D_2) appeared to show such a large amount of recrossing of even the variational transition state at energies near threshold.[25]

The trends for surface P are very similar to those of the JW surface.

The trends for surface M are similar to those for surface P except that there appears to be a significant recrossing effect for energies of 15 kcal/mol and above. The results in this case are similar to those for Cl + H_2 and isotopic analogs, with the accurate rate constant underestimated at low T due to insufficient tunneling at low E and overestimated at high T due to significant recrossing at high E.[17,18]

In addition to the errors treating tunneling dynamics and by the no-recrossing assumption, the results are quantitatively affected by the Morse I approximation for the stretches. Our experience with other collinear atom-diatom reactions[26] leads us to believe that the quantitative errors in Table II would generally be smaller if we used the WKB approximation to estimate the local zero-point energy of the stretching vibrations of the generalized transition states. Nevertheless we present results here

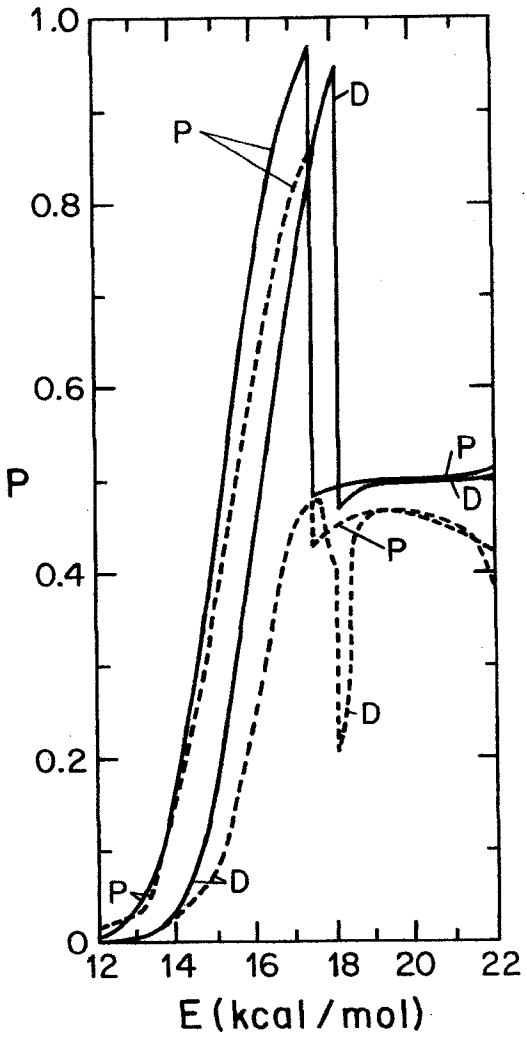

FIG. 4. Same as Fig. 2 except for potential energy surface D, for which the integrand peaks at 13.0, 14.5, and 16.05 kcal/mol and for potential energy surface P, for which the integrand peaks are at 10.5, 13.1, and 15.1 kcal/mol.

for the Morse I approximation because it is a general treatment of anharmonicity that can be applied even to polyatomic combustion reactions with ease.[27]

4.2 *Three-Dimensional Reaction*

The new degrees of freedom introduced in proceeding from a collinear to a three-dimensional world are the bends and rotations. Table III shows the harmonic and harmonic-plus-quartic approximations to the bending frequencies and zero-point energies at the saddlepoint and at the ICVT variational transition state for the three-dimensional reaction at 400 K. The effect of anharmonicity on the bending zero-point energy is about 0.1 kcal/mol. Variational optimization of the location of the generalized transition state has only a small effect on the bending frequency.

The barrier-height quantities characterizing the five surfaces are tabulated in Table III. This table includes the classical barrier height at the saddlepoint, $V^{\ddagger}$, the same quantity corrected for the difference in zero-point energy of the conventional transition state and the reactants, $\Delta V_a^{\ddagger G}$, and the height of the vibrationally adiabatic ground-state potential barrier relative to reactants, ΔV_a^{AG}. Note that $\Delta V_a^{\ddagger G}$ and ΔV_a^{AG} are the values for the three-dimensional reaction as evaluated at the saddlepoint ($s = 0$) and at the low-temperature limit of the variational transition state, respectively.[28] Table III shows that for the various surfaces the effective ground-state barrier height is 0.05–0.37 kcal/mol higher than the value computed using saddlepoint information. The ratios of conventional transition state theory rate constants to the hybrid ICVT rate constants are similar in three dimensions and collinearly.

Table I gives the transmission coefficients. We see that the importance of reaction-path curvature persists in three dimensions, i.e., the MEPSAG results are much smaller than the ones calculated by the more reliable approximations. There are large differences between the collinear and three-dimensional transmission coefficients, with the largest differences being factors of 5–8 for the JW surface at 200 K. The differences are very significant for all surfaces even at room temperature. This comparison gives a quantitative error estimate for the method applied to the present reaction by Lee *et al.*,[8] which approximates three-dimensional transmission coefficients by collinear ones.

Table I indicates that the transmission coefficient

TABLE III

Frequencies (in cm^{-1}), energetic quantities (in kcal/mol), and calculated rate constants (in cm^3 $molecule^{-1}$ s^{-1}) for the three-dimensional reactions

Surface	Harmonic bend freq.[a]	Saddle-point zero-point bend energies[b]	Barriers $V^{\ddagger}$	Barriers $\Delta V_a^{G}(s)$[c]	$^{1000}_{400}E_a$ ICVT	$^{1000}_{400}E_a$ ICVT/G[d]	$k^{ICVT/G}(T)$ T = 400 K[d]	$k^{ICVT/G}(T)$ T = 300 K[d]
JW	725	2.07	12.5	10.70	11.0	9.5	1.9(−16)[e]	6.0(−18)
	732	2.22		10.75		9.1	2.9(−16)	1.2(−17)
SL	703	2.01	13.8	11.75	12.3	10.6	5.9(−17)	1.5(−18)
	733	1.96		11.91		10.6	5.3(−17)	1.7(−18)
D	478	0.68	13.4	11.10	11.9	10.4	1.1(−16)	2.7(−18)
	463	0.75		11.38		10.9	6.9(−17)	1.4(−18)
P	513	0.73	12.6	10.45	11.1	9.6	2.3(−16)	8.7(−18)
	523	0.80		10.80		10.0	1.5(−16)	5.7(−18)
M	514	0.73	12.6	10.49	11.2	9.7	2.1(−16)	7.3(−18)
	524	0.80		10.86		10.0	1.5(−16)	5.9(−18)

[a]Upper entry is evaluated at the saddlepoint; lower entry is evaluated at the ICVT bottleneck at 400 K.

[b]Upper entry is harmonic; lower entry is a perturbation-variation solution to a fitted harmonic-quartic potential.

[c]Upper entry is evaluated at the saddlepoint ($s = 0$); lower entry is evaluated at the maximum of the three-dimensional ground-state adiabatic barrier ($s = s_*^{AG}$).

[d]Upper entry is for tunneling included by the SCTSAG method; lower entry is for tunneling included by the LAG method.

[e]Numbers in parenthesis are powers of ten.

is always larger for the three-dimensional reaction than the collinear one; this is consistent with what we found in several such comparisons presented earlier.[19] Table I also implies that most of the three-dimensional reaction proceeds by tunneling, even at temperatures of 400 K. This may be quantified by computing the percentage of ground-state reaction that proceeds by tunneling, as defined in ref. 19. For example, we find for surface P in the LAG approximation that this percentage is 99.89, 92, 71, 43, 30, and 23 for temperatures of 200, 300, 400, 600, 800, and 1000 K respectively. These percentages are even larger for the JW and SL surfaces.

The most recent evaluation[29] of experimental data for the O + H_2 reaction concludes that for T ≥ 400 K the expression of Baulch *et al.*,[30] namely

$$k = 3.0 \times 10^{-14}\, T \exp(-4480/T) \qquad (2)$$

fits most of the data within experimental error. (All rate constants are in cm^3 $molecule^{-1}$ s^{-1}.) At 1400 K, all ten calculated values of k, i.e., both ICVT/SCTSAG and ICVT/LAG calculations for all five surfaces, give values in the range 1.08×10^{-12} to 1.99×10^{-12}, and all these values agree within experimental error with the value of 1.71×10^{-12} computed from eq. (2).

Fitting the Arrhenius expression to the present theoretical rate constants at 400 and 1000 K yields the activation energies in columns 6 and 7 of Table III. Neglecting tunneling raises the energy of activation by 1.0–1.9 kcal/mol, even over the relatively high temperature range of 400–1000 K. The ICVT activation energies all agree with the vibrationally adiabatic ground-state barrier heights, ΔV_a^{AG}, within 0.5 kcal/mol, but including tunneling makes the computed activation energies 0.5–1.6 kcal/mol lower than ΔV_a^{AG} in every case. Comparing column 7 of Table III to the "experimental" value of 10.1 kcal/mol, from Equation (2) at 400 and 1000 K, shows that, for at least one of the two methods of including tunneling, each of the surfaces yields an activation energy within 0.6 kcal/mol or better of the experimental value; this is within experimental error.

The last two columns of Table III give the calculated rate constants at 400 and 300 K. Equation (2) yields 1.6×10^{-16} at 400 K and Dubinsky and McKenney's fit[31] to data obtained by the air afterglow method yields 2.4×10^{-16}. The only surface for which the predictions definitely disagree with experiment at 400 K is the SL one. The experimental data shows more scatter at lower temperatures,[29,31–33] but it appears that we may have underestimated the extent of tunneling. Such an underestimate would be consistent with the fact that when we study collinear reactions we usually find that the approximate methods underestimate the amount of tunneling for a given potential energy surface as compared to accurate quantal dynamics.[17–20,34]

Acknowledgments

The authors are grateful to Alan W. Magnuson for assistance with some of the calculations and to Joel M. Bowman and Albert F. Wagner for supplying potential subprograms, preprints, data, and many helpful discussions. The work at the University of Minnesota was supported in part by the United States Department of Energy, Office of Basic Energy Sciences, under contract no. DE-AC0279ER10425. The work at Chemical Dynamics Corporation was supported by the U.S. Army through the Army Research Office under contract no. DAAG-29-81-C-0015.

REFERENCES

1. Walch, S. P., Wagner, A. F., Schatz, G. C., and Dunning, T. H., Jr.,: J. Chem. Phys. 72:2894 (1980).
2. Wagner, A. F., Schatz, G. C., and Bowman, J. M.: J. Chem. Phys. 74, 4960 (1981).
3. Schatz, G. C., Wagner, A. F., Walch, S. P., and Bowman, J. M.: J. Chem. Phys. 74, 4984 (1981).
4. Bowman, J. M. and Lee, K. T.: *Potential Energy Surfaces and Dynamics Calculations* (D. G. Truhlar, Ed.), p. 359, Plenum, 1981.
5. Dunning, T. H., Jr., Walch, S. P., and Wagner, A. F.: *Potential Energy Surfaces and Dynamics Calculations* (D. G. Truhlar, Ed.), p. 329, Plenum, 1981.
6. Bowman, J. M., Ju, G.-Z., Lee, K. T., Wagner, A. F., and Schatz, G. C.: J. Chem. Phys. 75, 141 (1981).
7. Lee, K. T., Bowman, J. M., Wagner, A. F., and Schatz, G. C.: J. Chem. Phys. 76, 3563 (1982).
8. Lee, K. T., Bowman, J. M., Wagner, A. F., and Schatz, G. C.: J. Chem. Phys. 76, 3583 (1982).
9. Johnson, B. R. and Winter, N. W.: J. Chem. Phys. 66, 4116 (1977).
10. Schinke, R. and Lester, W. A., Jr.: J. Chem. Phys. 70, 4893 (1979).
11. Whitlock, P. A., Muckerman, J. T., and Fisher, E. R.: *Theoretical Investigations of the Energetics and Dynamics of the Reaction of* $O(^3P,^1D) + H_2$ *and* $C(^1D) + H_2$. Report from Research Institute for Engineering Sciences, Wayne State University, 1976.
12. Walch, S. P., Dunning, T. H., Jr., Bobrowicz, F. W., and Raffenetti, R.: J. Chem. Phys. 72, 406 (1980).
13. Johnston, H. S.: *Gas-Phase Reaction Rate Theory*, Ronald, 1966.

14. GARRETT, B. C. AND TRUHLAR, D. G.: J. Am. Chem. Soc. 101, 4534 (1979).
15. GARRETT. B. C., TRUHLAR, D. G., AND MAGNUSON, A. W.: J. Chem. Phys. 76, 2321 (1982).
16. HUBER, K. P. AND HERZBERG, G.: *Constants of Diatomic Molecules*, p. 508, Van Nostrand Reinhold, 1979.
17. GARRETT, B. C., TRUHLAR, D. G., GREV, R. S., AND MAGNUSON, A. W.: J. Phys. Chem. 84, 1730 (1980), 87, 4554(E) (1983).
18. GARRETT, B. C. AND TRUHLAR, D. G.: J. Phys. Chem. 83, 1079 (1979), 84, 682(E) (1980), 87, 4553(E) (1983).
19. SKODJE, R. T., TRUHLAR, D. G., AND GARRETT, B. C.: J. Chem. Phys. 77, 5955 (1982).
20. GARRETT, B. C. AND TRUHLAR, D. G.: J. Chem. Phys. 79, 4931 (1983).
21. GARRETT, B. C. AND TRUHLAR, D. G.: J. Phys. Chem. 83, 1915 (1979).
22. GARRETT, B. C. AND TRUHLAR, D. G.: J. Chem. Phys. 72, 3260 (1980).
23. GARRETT, B. C. AND TRUHLAR, D. G.: J. Am. Chem. Soc. 101, 4534 (1979).
24. GARRETT, B. C. AND TRUHLAR, D. G.: J. Am. Chem. Soc. 101, 5207 (1979).
25. GARRETT, B. C., TRUHLAR, D. G., GREV, R. S., MAGNUSON, A. W., AND CONNOR, J. N. L.: J. Chem. Phys. 73, 1721 (1980).
26. GARRETT, B. C. AND TRUHLAR, D. G.: J. Chem. Phys. 81, 309 (1984).
27. ISAACSON, A. D. AND TRUHLAR, D. G.: J. Chem. Phys. 76, 1380 (1982).
28. GARRETT, B. C., TRUHLAR, D. G., AND GREV, R. S.: *Potential Energy Surfaces and Dynamics Calculations* (D. G. Truhlar, Ed.), p. 587, Plenum, 1981.
29. COHEN, N. AND WESTBERG, K.: J. Phys. Chem. Ref. Data 12, 531 (1983).
30. BAULCH, D. L., DRYSDALE, D. D., HORNE, D. G., AND LLOYD, A. C.: Evaluated Kinetic Data for High-Temperature Reactions, Vol. 1, p. 49, Butterworths, 1972.
31. DUBINSKY, R. N. AND MCKENNEY, D. J.: Can. J. Chem. 53, 3531 (1975).
32. CAMPBELL, I. M. AND HANDY, B. J.: J. Chem. Soc. Faraday Trans. I, 74, 316 (1978).
33. LIGHT, G. C. AND MATUSUMOTO, J. H.: Int. J. Chem. Kinet. 12, 451 (1980).
34. GARRETT, B. C. AND TRUHLAR, D. G.: Proc. Natl. Acad. Sci. U.S.A. 76, 4755 (1979).

COMMENTS

N. J. Brown, Lawrence Berkeley Laboratory, USA. Your computed rate coefficients are very sensitive to reaction path curvature. How well do you need to know details of the potential energy surface along the minimum energy path to reliably determine reaction path curvature?

Authors' Reply. In order to determine accurately the reaction-path curvature along the minimum energy path (MEP) it is first necessary to find the MEP accurately. To accomplish this we have found it necessary to use a very small step size in the gradient-following algorithm. Typically we use step sizes in the range (1–5) $\times$ 10^{-4} a_0 and in the present calculation we used 10^{-4} a_0. Although we have not made a quantitative assessment of these effects, in a previous paper[1] we have shown the effect of smoothing the MEP upon the reaction-path curvature in the O + H_2 reaction.

REFERENCE

1. SKODJE, R. T., TRUHLAR, D. G., GARRETT, B. C.: J. Chem. Phys. 77, 5955 (1982).

•

A. Wagner, Argonne National Laboratory, USA. J. Bowman [IIT] and myself have used reduced dimensionality calculations on the rate constant using essentially the same Mod POLCI potential energy surface and have arrived at very comparable agreement to the same experimental measurements of the rate constants and isotope effects. Reduced dimensionality calculations blend exact quantum rate constant calculations in reduced dimensions (in this case the collinear OH and HH distances) into adiabatic treatments of the other degrees of freedom (in this case the bend) to arrive at a value for the fully dimensional rate constant. The convergence of these calculations, the variational transition state calculations, and experimental appears to have occurred over a large temperature range for $O(^3P)$ + $H_2(D2)$.

One question is whether the vibrationally excited rate $O(^3P)$ + $H_2(v = 1)$ has been calculated for comparison to Light's experiments (?). Reduced dimensionality calculations show significant sensitivity to the potential energy surface and show good agreement with the experiment for the Mod POLCI surface.

Authors' Reply. We have recently computed rate constants for the O + $H_2(n = 1) \rightarrow$ OH + H reaction using the VTST methods described elsewhere.[1] The Morse approximation for stretching vibrational energies used for thermal rate constants in the present paper is often inadequate for excited state rate constants so we used the WKB approximation instead. Otherwise, the methods used for the excited-state rate constants are the same as those used in the present paper and they include transmission coefficients which incorporate an anharmonic treatment of the bending degree of freedom. The results of these calculations are shown in the following table.

	$k^{ICVT/G}$ (T = 300 K) (cm^3 $molecules^{-1}$ s^{-1})	
Surface	SCTSA	LA
JW	3.2(−14)	4.1(−14)
SL	1.0(−14)	3.0(−14)
P	1.0(−14)	1.0(−14)
M	8.1(−15)	7.7(−15)

Light[2] has measured this rate constant at 300 K to be $(1.0^{+0.9}_{-0.6}) \times 10^{-14}$ cm^3 $molecule^{-1}$ s^{-1}. The only surface which definitely disagrees with experiment at 300 K is the JW one. These results are slightly different than those of Lee et al.[3] In their calculations, rate constants were obtained using conventional transition state theory with a harmonic treatment of stretch and bend vibrations and a transmission coefficient based upon quantum scattering on the non-bend-corrected collinear potential. Their calculations indicated that surfaces JW, SL, P, and M agreed well with experiment at 300 K but that surface D predicted a rate constant at 300 K which was too large by almost three orders of magnitude.

REFERENCES

1. Garrett, B. C. and Truhlar, D. G.: J. Chem. Phys. 81, 309 (1984).
2. Light, G. C.: J. Chem. Phys. 68, 2831 (1978).
3. Lee, K. T., Bowman, J. M., Wagner, A. F., and Schatz, G. C.: J. Chem. Phys. 76, 3583 (1982).